



OPEN ACCESS

EDITED BY
Muhsan Ehsan,
Bahria University, Pakistan

REVIEWED BY
Huiyuan Xu,
Sinopec, China
Chenglin Liu,
China University of Petroleum, Beijing,
China

*CORRESPONDENCE
Li Xu,
xuli0055@126.com

SPECIALTY SECTION
This article was submitted to
Geochemistry,
a section of the journal
Frontiers in Earth Science

RECEIVED 02 October 2022
ACCEPTED 31 October 2022
PUBLISHED 13 January 2023

CITATION
Xing L and Xu L (2023), Contribution of
soluble organic matter to hydrocarbon
generation in saline lacustrine source
rocks: Evidence from thermal
simulation experiments.
Front. Earth Sci. 10:1059948.
doi: 10.3389/feart.2022.1059948

COPYRIGHT
© 2023 Xing and Xu. This is an open-
access article distributed under the
terms of the [Creative Commons
Attribution License \(CC BY\)](https://creativecommons.org/licenses/by/4.0/). The use,
distribution or reproduction in other
forums is permitted, provided the
original author(s) and the copyright
owner(s) are credited and that the
original publication in this journal is
cited, in accordance with accepted
academic practice. No use, distribution
or reproduction is permitted which does
not comply with these terms.

Contribution of soluble organic matter to hydrocarbon generation in saline lacustrine source rocks: Evidence from thermal simulation experiments

Lantian Xing¹ and Li Xu^{2*}

¹Research Center for Oil and Gas Resources, Northwest Institute of Eco-Environment and Resources, Chinese Academy of Sciences, Lanzhou, China, ²Research Institute of Petroleum Exploration and Development Northwest, Petro China, Lanzhou, China

Soluble organic matter generally exists in the source rocks of saline lacustrine basins. In this paper, we quantified the contribution of soluble organic matter to hydrocarbon generation based on thermal simulation experiments using a saline lacustrine source rock from the Qaidam Basin. Our results show that the yields of gaseous and liquid hydrocarbons in the thermal simulation products are greatly improved in the presence of soluble organic matter. As a comparison, the maximum yields of gaseous and liquid hydrocarbons in series C (without soluble organic matter) were 270 mg/gTOC and 329.78 mg/gTOC, respectively, while in series A (with soluble organic matter) they were 364 and 602.98 mg/gTOC, respectively. The proportion of isoprenoids and n-alkanes in the products also increased from approximately 3%–40%. Meanwhile, the presence of soluble organic matter reduced the temperature corresponding to the hydrocarbon generation peak from 375 to 250°C. Moreover, the presence of soluble organic matter also had a remarkable change on the stable carbon isotope composition of methane, resulting in more ¹²C enrichment with a range of 2.24%–5.25%. The combined evidence indicates that soluble organic matter can promote the formation of immature–low maturity oil in source rocks.

KEYWORDS

saline lacustrine, soluble organic matter, thermal simulation experiment, source rock, Qaidam basin

Introduction

The exploration and development of conventional and non-conventional hydrocarbons are significant and essential for the economy and growth of a country (Aziz et al., 2020; Khalil Khan et al., 2022). Due to the shortage of conventional resources, academics and geoscientists have to consider unconventional resources or reassess source rocks with low total organic carbon (TOC) content (Pan et al., 2010; Guo et al., 2019; Xing et al., 2022). The Paleogene (E) in the western Qaidam basin is widely distributed saline

TABLE 1 Mineral composition data of source rock sample (%).

Quartz	Orthoclase	Plagioclase	Calcite	Siderite	Pyrite	Anhydrite	Augite	Dolomite	Clay minerals
13.8	1.4	10.4	12	0.4	4	1.7	4.9	25.9	25.5

lacustrine source rocks. However, the source rocks are generally not considered rich in organic matter and are much less abundant than the typical lacustrine source rock. In the past 5 years, the significant hydrocarbon exploration discovery has sped up studying the re-evaluation of this saline lacustrine source rocks (Guo et al., 2019).

According to previous studies, soluble organic matter is found in this saline lacustrine source rocks in the western Qaidam Basin (Zhang et al., 2017), which has an impact on the hydrocarbon potential and generation process of such source rocks (Du et al., 2021; Guan et al., 1998). In addition, this soluble organic matter is the parent material of middle-shallow hydrocarbon reservoirs in this area. Hence, the study of soluble organic matter in different occurrence states in source rocks is of great significance in re-evaluating the hydrocarbon potential and generation process of organic matter (Pan et al., 2018; Guan et al., 1998). Few previous works have been carried out on the hydrocarbon generation potential and evaluation of this set of source rocks (Zhang et al., 2017). However, an assessment of the quantitative contribution of soluble organic matter to hydrocarbon generation in saline lacustrine source rocks is still lacking. Given the above reasons, a comparative hydrocarbon-generation thermal simulation experiment was designed in this study. The primary purpose is to reevaluate and quantify the role and contribution of soluble organic matter in the hydrocarbon generation process within saline lacustrine source rocks. Additionally, the quantitative study based on thermal simulation experiments provides reliable evidence for re-evaluation of the potential resources in this area and subsequent exploration.

Samples and methods

Sample preparation

The experimental sample was collected from the V sand unit of the upper member of the lower Ganchaigou Formation. The sample was washed and pulverized to 100-mesh and then divided into three equal-weight parts (series A–C). The series A sample comprised source rock containing kerogen, and free and combinative soluble organic matter. The series B sample was extracted with chloroform for 72 h to remove free soluble organic matter; hence, this sample contained only kerogen and combinative organic matter. Series C underwent chloroform

TABLE 2 TOC and pyrolysis parameters of sub-samples.

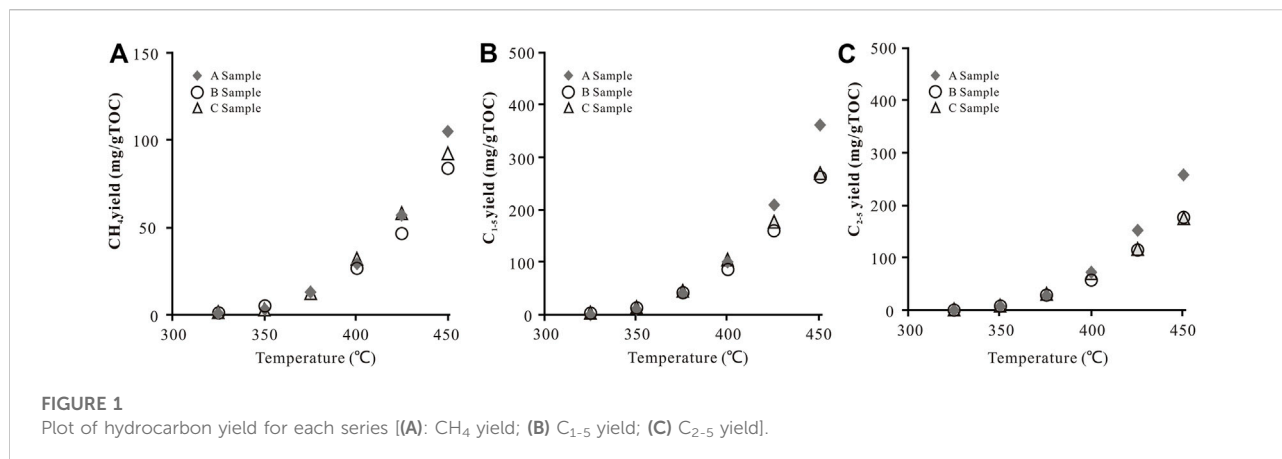
Sub-samples	TOC (%)	S ₁ (mg/g)	S ₂ (mg/g)	T _{max} (°C)
Series A	1.4	2.6	5.5	427.7
Series B	1.1	0.5	5.4	423.9
Series C	17.2	22.1	65.0	424.8

extraction and removal of combinative organic matter, so that only kerogen remained. After sample pretreatment, an ELTRA CSI analyzer and a Rock-Eval 6 pyrolysis analyzer were used to measure the total organic carbon (TOC), S₁, S₂, and T_{max} values. The mineral composition of the source rock sample is shown in Table 1, while the TOC and pyrolysis parameters are shown in Table 2. The high dolomite and low clay mineral contents indicate that the sample is a typical saline lacustrine source rock.

Thermal simulation experiments and product analysis

Thermal simulation experiments were conducted using an autoclave–gold tube system. Details of the thermal simulation experimental process can be found in previous research (Xiao et al., 2005, 2006; Pan et al., 2012; Jin et al., 2013; Li et al., 2013). Briefly, in these experiments, the pressure was set as 50 MPa, and the pressure program controlled its change by ± 0.1 MPa. After the autoclave was rapidly raised from room temperature to 250°C, it was further raised to 450°C at a heating rate of 2°C/h. A sample was taken every 25°C between 250 and 450°C, and pyrolysis data of different temperature points were obtained for each series (A–C). The pyrolysis experiments were completed simultaneously so that the experimental conditions of the series A–C samples were utterly consistent.

After each thermal simulation experiment, each gold tube was put into a vacuum glass acquisition system connected to a chromatograph (Tian et al., 2006; Guo et al., 2009), and the gold tube was punctured. Once the gas was balanced, the valve was opened, and the gas was automatically imported into an HP5890 II chromatograph for quantitative analysis. The gas chromatograph was equipped with a fused silica column (Poraplot-Q, 30 m \times 0.25 mm \times 0.25 μ m) with Helium as the carrier gas at a constant flow rate of 1.2 ml/min. The initial gas chromatograph (GC) oven temperature was 60°C for 6 min,



followed by an increase of 15°C/min up to 180°C and maintenance for 4 min. The minimum detection limit of the system is 0.01 ml gas, and the relative error is <0.5% (Pan et al., 2012; Jin et al., 2013; Li et al., 2013).

The gas chromatograph-isotope ratio-mass spectrometer (GC-IR-MS) analysis of the gas in this study was performed on a Delta Plus^{XL} equipped with a GC. The GC was fitted with the same column as described above, and the GC temperature program was as follows: start temperature of 50°C, held for 3 min, followed by an increase gradient of 3°C/min to 200°C (Guo et al., 2009) and a final hold time of 30 min. Individual compounds were oxidized at 930°C for measurement of their carbon isotope ratios.

Liquid hydrocarbon products were extracted with dichloromethane, filtered with a filter membrane (pore size 0.45 μm), and weighed. Hydrocarbons were then identified using a GC/MS system (Agilent 7890, Agilent Technologies, United States) interfaced with a mass spectrometric detector (Xia et al., 2013) (MSD, Agilent 5973N). Helium was used as the carrier gas in constant (Behar et al., 1992) flow mode at 2 ml/min. The injector temperature was 280°C, and the oven temperature program was 3 min at 40°C, followed by an increase of 2°C/min up to 100°C, then 5°C/min up to 280°C, where it was maintained for 20 min. The ionization energy was 70 eV.

Results and discussion

Productivity and stable carbon isotope composition of gases

Hydrocarbon gas yields and stable carbon isotope compositions at different simulation temperatures are shown in Figure 1 and Table 3. When the simulated temperature was lower than 375°C, the gaseous hydrocarbon yields of the three series were similar, because the samples had not wholly entered the pyrolysis gas production stage. A large number of minerals in series A

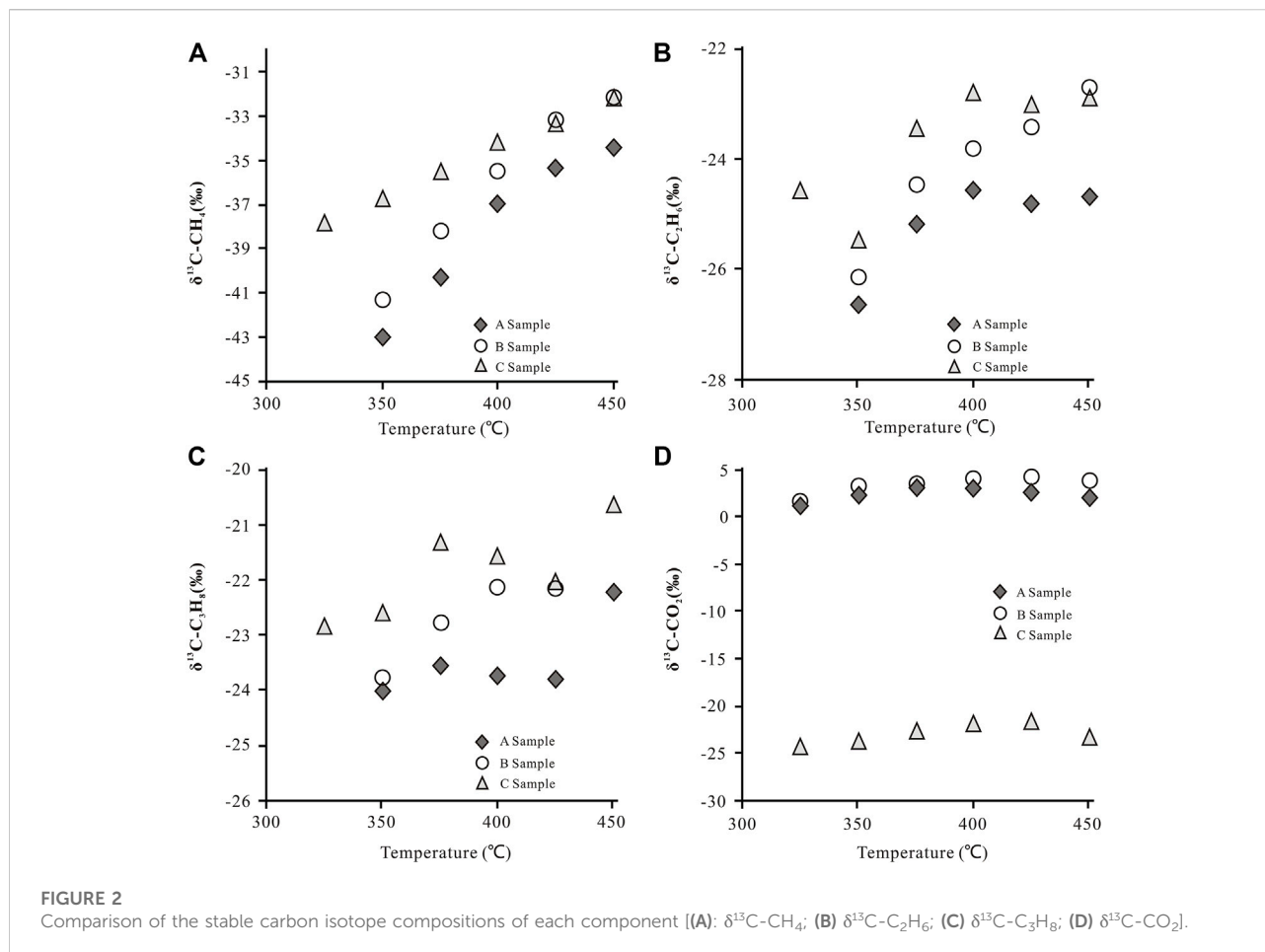
affected the hydrocarbon generation of organic matter. When the experimental temperature reached 400°C, the hydrocarbon gas yield of the series A sample was considerably higher than those of series B and C. This indicates that the soluble organic matter had begun to produce hydrocarbon gases. As the simulated temperature rose, the role of soluble organic matter became more significant. For example, at 450°C, the total hydrocarbon gas (C₁₋₅) yield of series A was 364 mg/gTOC, while the series B and C yields were 262.56 and 270 mg/gTOC, respectively. In addition, the yield data (Figure 1 and Table 3) also show that the methane and (Wang and Cheng, 2000) total hydrocarbon gas yields of the B series sample were similar to those of the C series. In contrast, the liquid hydrocarbon yield (C₆₋₁₄) of the B series sample was higher than that of the C series, indicating that the contribution of bound organic matter to the hydrocarbon products is mainly reflected in the liquid hydrocarbons.

Figure 2 shows the stable carbon isotope compositions of methane (Figure 2A), ethane (Figure 2B), and propane (Figure 2C) in the three series. The isotopic composition of each series became markedly heavier with an increase in temperature. Compared with series C, the carbon isotope compositions of methane, ethane, and propane in series A were markedly enriched in ¹²C. However, for carbon dioxide (Figure 2D), the products in series C were more enriched in ¹²C than those in series A and B.

On the basis of the above experimental results, the differences in gas yield and isotopic characteristics of each series are inferred to be caused by the type and quantity of organic matter in the samples themselves, which leads to different gas production mechanisms and processes. The series A sample contained kerogen and soluble organic matter, and its hydrocarbon production per unit of organic matter was higher than those of series B and C. This is a result of the contribution of soluble organic matter in series A. The differences in carbon isotope signatures are related to the different gas production mechanisms. Gas produced in series C mainly came from kerogen cracking, primarily derived from the demethylation of C₁₄₊ nuclear polycondensation. In the series A sample, in addition to

TABLE 3 Hydrocarbon yields (mg/gTOC) and stable carbon isotope compositions (‰) for the A, B, and C series samples at different temperatures.

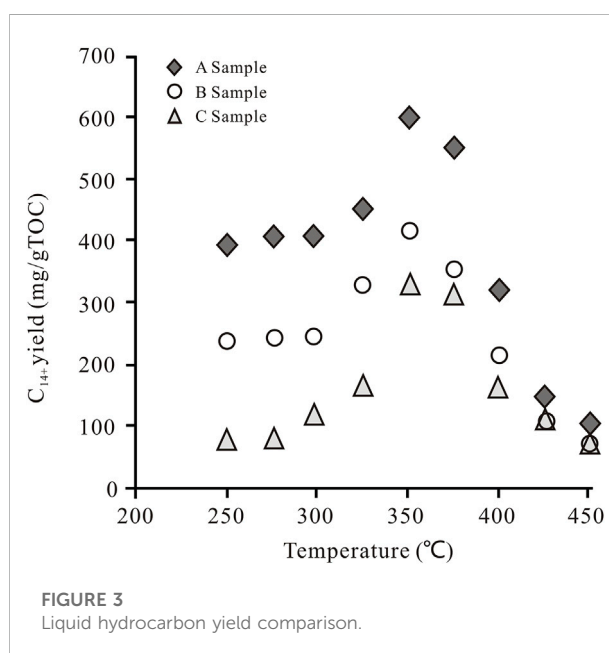
T (°C)	Weight (mg)	EasyRo (%)	CH ₄	C ₂ H ₆	C ₂ H ₄	C ₃ H ₈	C ₃ H ₆	iC ₄ H ₁₀	nC ₄ H ₁₀	iC ₅ H ₁₂	nC ₅ H ₁₂	C _{6–14}	C ₁₄₊	C _{1–5}	C _{2–5}	δ ¹³ C			
																CH ₄	C ₂ H ₆	C ₃ H ₈	CO ₂
A Sample																			
250.1	700.12	0.31	0.11	0.03	0.00	0.03	0.00	0.00	0.01	0.00	0.00	2.25	394.83	0.20	0.09	n.d.	n.d.	n.d.	−1.02
275.1	700.29	0.36	0.20	0.09	0.01	0.11	0.01	0.01	0.01	0.01	0.00	2.91	409.01	0.45	0.25	n.d.	n.d.	n.d.	0.02
298.4	700.52	0.43	0.29	0.07	0.04	0.09	0.02	0.05	0.03	0.01	0.01	4.08	409.90	0.63	0.34	n.d.	n.d.	n.d.	0.64
325.0	700.53	0.53	0.94	0.32	0.01	0.46	0.04	0.18	0.14	0.06	0.03	9.55	453.74	2.17	1.23	n.d.	n.d.	n.d.	1.22
350.1	700.10	0.64	4.18	2.23	0.01	2.96	0.06	0.73	1.10	0.47	0.28	24.31	602.98	12.03	7.85	−42.98	−26.61	−23.99	2.32
375.1	700.04	0.74	13.58	9.06	0.02	10.50	0.08	2.24	4.10	1.67	1.18	92.70	557.11	42.42	28.84	−40.22	−25.17	−23.53	3.10
400.1	700.28	0.89	29.77	22.20	0.01	25.73	0.11	5.74	11.11	4.62	3.45	220.04	323.34	102.74	72.97	−36.89	−24.55	−23.73	2.98
425.1	620.00	1.13	56.79	44.76	0.02	54.15	0.25	12.57	24.44	9.39	7.45	231.97	148.96	209.81	153.02	−35.29	−24.79	−23.79	2.68
450.1	499.83	1.40	104.77	85.19	0.04	97.63	0.40	21.94	37.78	8.82	7.66	79.71	105.75	364.24	259.47	−34.35	−24.68	−22.19	2.07
B Sample																			
250.1	699.89	0.31	0.20	0.10	0.01	0.11	0.01	0.02	0.03	0.02	0.01	2.01	239.38	0.50	0.3	n.d.	n.d.	n.d.	−0.14
275.1	700.15	0.36	0.33	0.19	0.04	0.26	0.01	0.02	0.03	0.02	0.02	3.64	248.29	0.93	0.6	n.d.	n.d.	n.d.	0.72
298.4	699.91	0.43	0.54	0.28	0.04	0.40	0.03	0.07	0.06	0.03	0.02	6.52	251.51	1.47	0.93	n.d.	n.d.	n.d.	0.84
325.0	700.12	0.53	1.21	0.41	0.01	0.54	0.04	0.16	0.16	0.06	0.14	13.2	333.15	2.73	1.52	n.d.	n.d.	n.d.	1.82
350.1	700.19	0.64	5.00	2.65	0.02	3.28	0.07	0.71	1.21	0.48	0.34	30	420.34	13.76	8.76	−41.28	−26.13	−23.75	3.43
375.1	700.37	0.74	13.75	9.75	0.02	10.36	0.08	2.02	4.03	1.41	1.22	60.7	361.68	42.63	28.88	−31.88	−24.44	−22.76	3.63
400.1	699.47	0.89	27.43	19.81	0.02	19.54	0.16	4.58	7.94	3.18	3.55	106.85	217.96	86.22	58.79	−35.45	−23.80	−22.10	4.08
425.1	600.11	1.13	47.27	37.38	0.03	41.45	0.23	9.18	13.74	6.96	6.31	113.02	112.94	162.55	115.28	−33.07	−23.40	−22.14	4.22
450.1	499.84	1.40	84.82	63.67	0.04	66.86	0.42	14.62	23.20	4.83	4.09	67.19	72.63	262.56	177.74	−32.12	−22.68	−19.93	3.92
C Sample																			
250.1	120.71	0.31	0.21	0.02	0.00	0.03	0.00	0.00	0.01	0.00	0.00	2.56	79.23	0.28	0.07	n.d.	n.d.	n.d.	−22.37
275.1	120.59	0.36	0.35	0.05	0.00	0.08	0.00	0.01	0.01	0.00	0.00	3.46	81.8	0.50	0.15	n.d.	n.d.	n.d.	−25.37
298.4	120.90	0.43	0.71	0.14	0.00	0.22	0.00	0.03	0.05	0.02	0.01	4.39	116.9	1.18	0.47	n.d.	n.d.	n.d.	−25.72
325.0	100.87	0.53	1.68	0.58	0.00	0.91	0.01	0.25	0.28	0.15	0.07	11.3	166.21	3.93	2.25	−37.73	−24.55	−22.81	−24.19
350.1	100.97	0.64	3.54	2.41	0.00	3.13	0.01	0.99	1.41	0.98	0.48	25.7	329.78	12.94	9.4	−36.67	−25.45	−22.56	−23.66
375.1	100.95	0.74	12.72	10.32	0.00	10.59	0.01	3.07	4.81	2.93	1.56	78.77	318.01	46.02	33.3	−35.42	−23.42	−21.29	−22.57
400.1	100.83	0.89	32.18	24.94	0.00	23.46	0.03	6.30	9.87	4.93	2.71	163.35	165.06	104.42	72.24	−34.08	−22.78	−21.55	−21.80
425.1	68.02	1.13	58.76	43.05	0.01	41.07	0.07	10.14	14.87	5.53	3.56	107.92	106.04	177.06	118.3	−33.28	−22.99	−22.00	−21.53
450.1	80.85	1.40	92.37	64.24	0.01	64.56	0.17	15.72	23.34	5.89	4.27	49.4	100.03	270.58	178.21	−32.11	−22.86	−20.62	−23.16

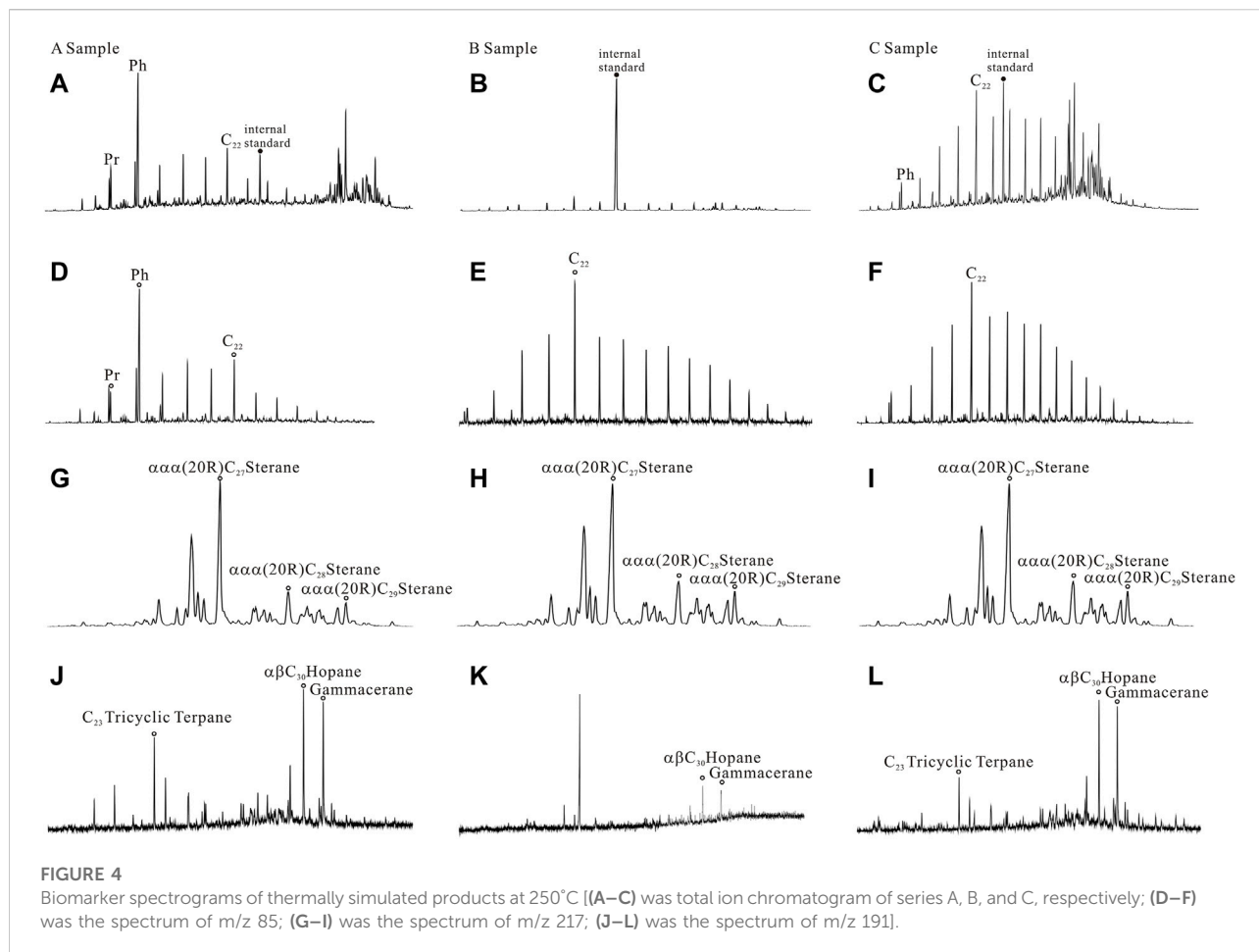


demethylation, the C–C bond of C_{6+} saturated chains and the C–C bond of C_{2-5} fatty chains was fractured in the cracking gas (Hill et al., 2003; Guo et al., 2009). The mean $\delta^{13}\text{C}$ value of carbon dioxide in series C was -23.37‰ (Figure 2D), while series A and B samples exhibited positive $\delta^{13}\text{C}$ values (Figure 2D) caused by the thermal cracking of inorganic minerals in the pyrolysis process. We can conclude that the abundant soluble organic matter in the source rocks of this saline lake basin has a significant influence on hydrocarbon generation, both in terms of gas generation potential and controlling the carbon isotope characteristics of hydrocarbon gases.

Hydrocarbon productivity

Liquid hydrocarbons were a fundamental component of the thermal simulation products. When the temperature was lower than 350°C , the liquid hydrocarbon yield increased slowly with an increase in experimental temperature. In comparison, when the temperature was higher than 350°C , the yield decreased gradually as





the temperature increased (Figure 3). In the three sample series analyzed herein, the variation trend of liquid hydrocarbon yield with changing temperature was consistent (Figure 3).

Although each series showed a similar change trend, the corresponding yields were markedly different at equivalent temperatures. At a given temperature condition, series A had the largest yield, and series C the smallest. These differences in liquid hydrocarbon yield further demonstrate the contribution of free and combinative soluble organic matter to hydrocarbon generation. The contribution of hydrocarbons generated by pyrolysis of combinative soluble organic matter results in the yield of series B being higher than that of series C. Moreover, concurrent pyrolysis of free and combinative soluble organic matter results in the yield of series A being the highest.

Biomarker characteristics

In addition to the yield and carbon isotope analysis of gaseous and liquid hydrocarbons, we also analyzed the characteristics of biomarkers (Figure 4). Because the total hydrocarbon production of series B was low, there was insufficient material to carry out GCMS

analysis and biomarker parameter calculation. Therefore, only the differences between the biomarkers of series A and C are discussed below.

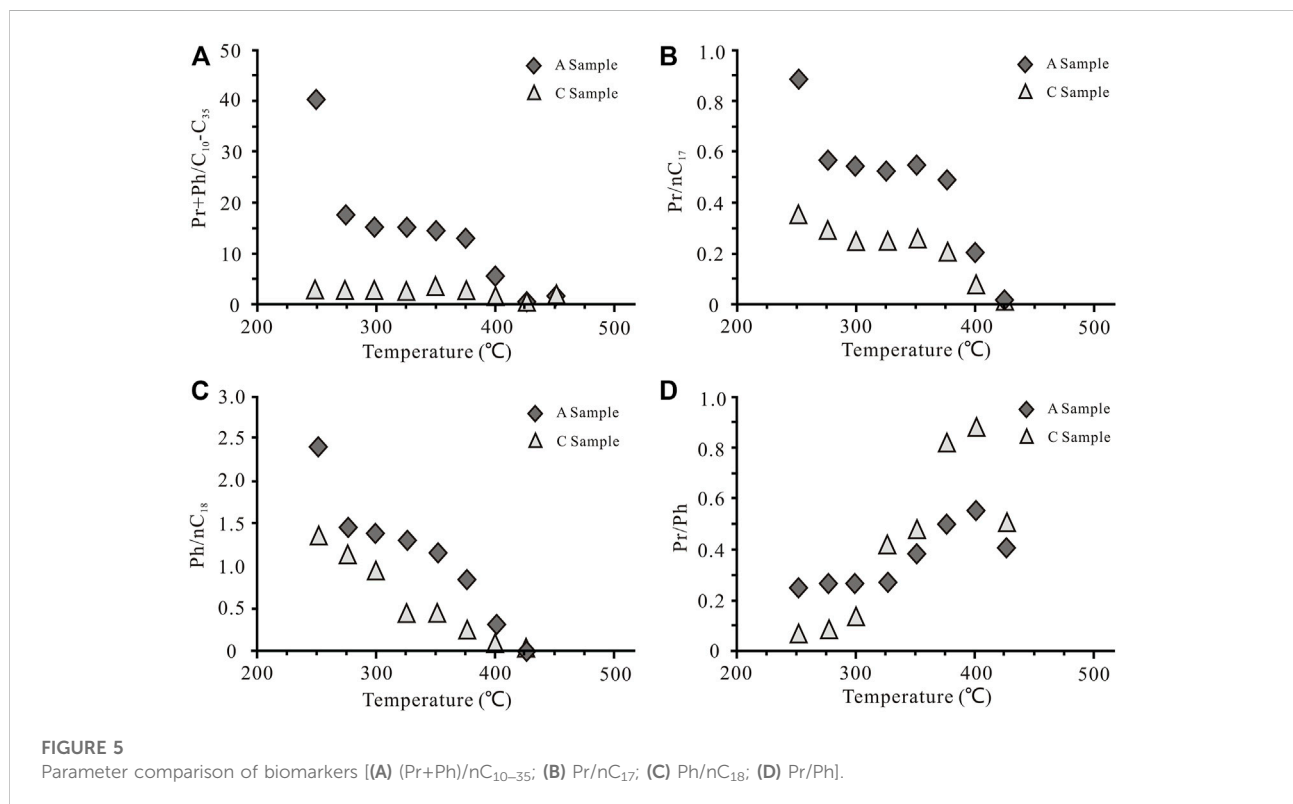
Both series A and C displayed abundant steranes at different temperatures, with the $\alpha\alpha\alpha C_{27}$ sterane having the highest concentration (Figures 4G,I). In addition, both samples contained abundant 4-methyl steranes (Figures 4G,I), which are related to a hydrocarbon generation parent material dominated by algae. Moreover, the mean value of gammacerane/ $\alpha\beta$ - C_{30} hopane was 0.93 in series A and 0.96 in series C (Figure 4J,L), indicating a high salinity sedimentary environment. The contents of tricyclic terpanes in the two series were relatively consistent, among which the C_{23} tricyclic terpene/ $(C_{23}$ tricyclic terpene + C_{30} hopane) of series A was 0.38, and that of series C was 0.26 (Figure 4J,L; Table 4). The above results indicate that the kerogen and soluble organic matter in these samples have the same parent material and source environment.

Although each of the series samples exhibited similar parent material and environment, the isoprenoid contents in the products were markedly different. As shown in Figures 4A,D, series A products contained high contents of Pr and Ph, and Ph was the dominant peak in the total ionization chromatograph.

TABLE 4 Characteristics of biomarkers in experimental series A and C.

	Temperature (°C)	$\frac{\sum C_{21-}}{\sum C_{22+}}$	Pr/Ph	Pr/nC ₁₇	Ph/nC ₁₈	A	B	C	D
Series A	250.1	1.76	0.23	0.89	2.46	0.40	0.93	6.74	0.38
	275.1	0.87	0.25	0.57	1.49	0.16	1.01	6.14	0.31
	298.4	0.76	0.24	0.54	1.42	0.14	0.96	6.25	0.31
	325.0	0.80	0.25	0.53	1.34	0.14	0.98	6.02	0.31
	350.1	0.86	0.35	0.55	1.19	0.13	1.05	6.62	0.37
	375.1	1.09	0.45	0.49	0.88	0.12	n.d.	6.21	0.69
	400.1	1.11	0.50	0.21	0.36	0.05	n.d.	5.46	0.96
	425.1	1.42	0.37	0.02	0.03	0.01	n.d.	5.50	1.00
	450.1	0.53	n.d.	n.d.	n.d.	0.02	n.d.	5.66	n.d.
	Series C	250.1	0.29	0.06	0.35	1.38	0.03	0.96	5.61
275.1		0.29	0.08	0.29	1.15	0.03	0.95	5.25	0.26
298.4		0.32	0.12	0.24	0.96	0.03	1.04	5.33	0.28
325.0		0.45	0.38	0.25	0.46	0.03	1.13	5.52	0.31
350.1		0.50	0.43	0.26	0.46	0.03	1.14	5.39	0.33
375.1		0.74	0.73	0.20	0.25	0.03	n.d.	4.32	0.85
400.1		0.90	0.79	0.08	0.09	0.01	n.d.	5.51	1.00
425.1		0.86	0.45	0.01	0.01	0.01	n.d.	5.95	1.00
450.1		0.28	0.82	0.27	0.51	0.01	n.d.	5.87	n.d.

Note: A, (Pr + Ph)/ $\sum C_{14-36}$; B, gammacerane/ $\alpha\beta C_{30}$ hopane; C, $\alpha\alpha C_{27}$ sterane/ $\alpha\alpha C_{29}$ sterane; D, C₂₃ tricyclic terpane/(C₂₃ tricyclic terpane + $\alpha\beta C_{30}$ hopane).



The ratio of (Pr+ Ph)/nC₁₀₋₃₅ in the product reached 40% at 250°C, but the ratio gradually decreased with increasing temperature. By comparison, the contents of Pr and Ph in the products of series C were markedly reduced (Figure 4C), and the ratio of (Pr+Ph)/nC₁₀₋₃₅ was only 1%–3% (Figure 5A; Table 4). Phytane dominance was observed in both series A and C, with Pr/nC₁₇ and Ph/nC₁₈ ratios of 0.89 and 2.46, and 0.35 and 1.38, respectively. However, with the simulated temperature increase, the ratio gradually approached zero owing to a large amount of isoprenoid cracking at high temperatures. This phenomenon is consistent with previous results (Xia et al., 1999).

Conclusion

On the basis of temperature-programmed simulation experiments of saline lacustrine low-maturity source rocks from the Qaidam Basin, the influence of soluble organic matter on the hydrocarbon generation process and isotopic characteristics of the resultant products were comparatively analyzed and discussed. The following conclusions can be drawn:

- (1) The presence of soluble organic matter substantially influences the hydrocarbon generation capacity, stable carbon isotope composition, and composition of liquid hydrocarbon biomarkers of source rocks. In addition to increasing the yield of hydrocarbons, the carbon isotope composition of the products is enriched in ¹²C, and the content of isoalkanes in liquid hydrocarbons is increased.
- (2) Soluble organic matter also influences the evolution of source rocks. Soluble organic matter can promote a large amount of hydrocarbon generation during the early stage of the thermal degradation of source rocks, thus forming large quantities of immature–low maturity oil and gas, and widening the hydrocarbon-generation range of source rocks.

References

- Aziz, H., Ehsan, M., Ali, A., Khan, H. K., and Khan, A. (2020). Hydrocarbon source rock evaluation and quantification of organic richness from correlation of well logs and geochemical data: A case study from the sembar formation, southern indus basin, Pakistan. *J. Nat. Gas. Sci. Eng.* 81, 103433. doi:10.1016/j.jngse.2020.103433
- Behar, F., Kressman, S., Rudkiewicz, J. L., and Vandenbrouke, M. (1992). Experimental simulation in a confined system and kinetic modeling of kerogen and oil cracking. *Org. Geochem.* 19 (1-3), 173–189. doi:10.1016/0146-6380(92)90035-V
- Du, P. Y., Cai, J. G., Liu, Q., Zhang, X. J., and Wang, J. (2021). A comparative study of source rocks and soluble organic matter of four sags in the Jiyang Depression, Bohai Bay Basin, NE China. *J. Asian Earth Sci.* 216 (15), 104822. doi:10.1016/j.jseae.2021.104822
- Guan, P., Xu, Y. C., and Liu, W. H. (1998). Quantitative estimates of different existing state organic matter in source rocks. *Chin. Sci. Bull.* 43 (14), 1556–1559. (in Chinese with English abstract).
- Guo, L. G., Xiao, X. M., Tian, H., and Song, Z. G. (2009). Distinguishing gases derived from oil cracking and kerogen maturation: Insights from laboratory pyrolysis experiments. *Org. Geochem.* 40 (10), 1074–1084. doi:10.1016/j.orggeochem.2009.07.007
- Guo, L., Xiao, X., Tian, H., and Song, Z. (2009). Distinguishing gases derived from oil cracking and kerogen maturation: Insights from laboratory pyrolysis experiments. *Org. Geochem.* 40, 1074–1084. doi:10.1016/j.orggeochem.2009.07.007
- Guo, P., Liu, C. Y., Wang, L. Q., Zhang, G. Q., and Fu, X. G. (2019). Mineralogy and organic geochemistry of the terrestrial lacustrine pre-salt sediments in the Qaidam basin: Implications for good source rock development. *Mar. Pet. Geol.* 107, 149–162. doi:10.1016/j.marpetgeo.2019.04.029
- Hill, R. H., Tang, Y., and Kaplan, I. R. (2003). Insights into oil cracking based on laboratory experiments. *Org. Geochem.* 34 (12), 1651–1672. doi:10.1016/S0146-6380(03)00173-6
- Jin, X. D., Li, E. T., Pan, C. C., Yu, S., and Liu, J. Z. (2013). Interaction of coal and oil in confined pyrolysis experiments: Insight from the yield and composition of gas hydrocarbons. *Mar. Pet. Geol.* 48, 379–391. doi:10.1016/j.marpetgeo.2013.09.002
- Khalil Khan, H., Ehsan, M., Ali, A., Amer, M. A., Aziz, H., Khan, A., et al. (2022). Source rock geochemical assessment and estimation of TOC using well logs and geochemical data of Talhar Shale, Southern Indus Basin, Pakistan. *Front. Earth Sc.-Switz.* 10, 969936. doi:10.3389/feart.2022.969936

Data availability statement

The original contributions presented in the study are included in the article/supplementary material, further inquiries can be directed to the corresponding author.

Author contributions

LaX: conceptualization, formal analysis, and writing-original draft. LiX: data curation, formal analysis, validation, writing-review and editing.

Conflict of interest

Author LiX was employed by the company Research Institute of Petroleum Exploration and Development Northwest, Petro China.

The remaining author declares that the research was conducted in the absence of any commercial or financial relationships that could be construed as a potential conflict of interest.

Publisher's note

All claims expressed in this article are solely those of the authors and do not necessarily represent those of their affiliated organizations, or those of the publisher, the editors and the reviewers. Any product that may be evaluated in this article, or claim that may be made by its manufacturer, is not guaranteed or endorsed by the publisher.

- Li, E. T., Pan, C. C., Yu, S., Jin, X. D., and Liu, J. Z. (2013). Hydrocarbon generation from coal, extracted coal and bitumen rich coal in confined pyrolysis experiments. *Org. Geochem.* 64, 58–75. doi:10.1016/j.orggeochem.2013.09.004
- Pan, C. C., Jiang, L. L., Liu, J. Z., Zhang, S. C., and Zhu, G. Y. (2012). The effects of pyrobitumen on oil cracking in confined pyrolysis experiments. *Org. Geochem.* 45, 29–47. doi:10.1016/j.orggeochem.2012.01.008
- Pan, C. C., Zhang, M., Peng, D. H., Yu, L. P., Liu, J. Z., Sheng, G. Y., et al. (2010). Confined pyrolysis of Tertiary lacustrine source rocks in the Western Qaidam Basin, Northwest China: Implications for generative potential and oil maturity evaluation. *Appl. Geochem.* 25, 276–287. doi:10.1016/j.apgeochem.2009.11.013
- Pan, Y. H., Li, M. W., Sun, Y. G., Li, Z. M., Jiang, Q. G., and Liao, Y. H. (2018). Geochemical characterization of soluble organic matter with different existing states in low-maturity argillaceous source rocks of lacustrine facies. *Geochim.* 47 (4), 335–344. (in Chinese with English abstract).
- Tian, H., Wang, Z. M., Xiao, Z. Y., Li, X. Q., and Xiao, X. M. (2006). Oil cracking to gases: Kinetic modeling and geological significance. *Chin. Sci. Bull.* 51 (22), 2763–2770. doi:10.1007/s11434-006-2188-8
- Wang, Z. Y., and Cheng, K. M. (2000). The organic geochemical characteristics comparison and contributors of different existing state organic matter in carbonate rocks. *Acta Sedimentol. Sin.* 18 (4), 600–605. (in Chinese with English abstract).
- Xia, X. Y., James, C., Braun, R., and Tang, Y. C. (2013). Isotopic reversals with respect to maturity trends due to mixing of primary and secondary products in source rocks. *Chem. Geol.* 339 (15), 205–212. doi:10.1016/j.chemgeo.2012.07.025
- Xia, Y. Q., Zhou, F. Y., Peng, D. H., and Meng, Q. X. (1999). Experimental simulation of immature-low mature oil formation in Qaidam Basin. *Nat. Gas. Geosci.* 10, 30–36. (in Chinese with English abstract).
- Xiao, X. M., Xiong, M., Tian, H., Wilkins, R. W. T., Huang, B. J., and Tang, Y. C. (2006). Determination of the source area of the ya13-1 gas pool in the qiongdongnan basin, south China sea. *Org. Geochem.* 37 (9), 990–1002. doi:10.1016/j.orggeochem.2006.06.001
- Xiao, X. M., Zeng, Q. H., Tian, H., Wilkins, R. W. T., and Tang, Y. C. (2005). Origin and accumulation model of the AK-1 natural gas pool from the Tarim Basin, China. *Org. Geochem.* 36 (9), 1285–1298. doi:10.1016/j.orggeochem.2005.04.001
- Xing, L. T., Xu, L., Zhang, P. Z., Zhang, J., and Wang, P. (2022). Organic geochemical characteristics of saline lacustrine source rocks: A case study from the yingxi area, Qaidam basin, China. *Geochem. Int.* 60 (1), 92–108. doi:10.1134/S00167029221150015
- Zhang, B., He, Y. Y., Chen, Y., Meng, Q. y., and Yuan, L. (2017). Geochemical characteristics and oil accumulation significance of the high quality saline lacustrine source rocks in the Western Qaidam Basin, NW China. *Acta Pet. Sin.* 38 (10), 1–10. (in Chinese with English abstract).